

Molecular Electronic Structure and Energetics of the Isomers of Ti₂H₆

Simon P. Webb and Mark S. Gordon*

Contribution from the Department of Chemistry, Iowa State University, Ames, Iowa 50011

Received September 11, 1997. Revised Manuscript Received January 12, 1998

Abstract: *Ab initio* calculations have been performed on five singlet and five triplet isomers which are minima on the two lowest potential energy surfaces of Ti₂H₆. We have used single-configuration ROHF as well as multiconfigurational methods, employing triple- ζ with polarization basis sets. Dynamic correlation effects are accounted for using second-order perturbation methods. Staggered and eclipsed C_{3v} triple hydrogen bridged structures, which have been studied previously using single-determinant closed-shell reference wave functions, are shown to require a more sophisticated treatment. The remaining isomers—C_s triple hydrogen bridged, D_{2h} double hydrogen bridged, and D_{4h} quadruple hydrogen bridged—have not previously been considered. The triplets are by definition diradical, and the singlets are found to possess largely diradical character. The D_{2h} isomer may be thought of as the simplest model for dititanium(III) bridged compounds. It is found to be antiferromagnetic with a calculated isotropic exchange interaction of $J = -250 \text{ cm}^{-1}$ (singlet–triplet gap of 1.43 kcal/mol). All Ti₂H₆ isomers are predicted to be lower in energy than the separated monomers: 2TiH₃. The lowest energy isomer is the triplet C_s structure with an exothermic dimerization energy of 56.4 kcal/mol on the classical ground-state potential energy surface.

I. Introduction

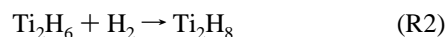
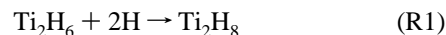
Titanium hydrides are an important class of compounds. Their catalytic behavior in many reactions, including polymerization of olefins and nitrogen fixation,¹ has ensured continuing interest and research both experimentally and theoretically. In addition to studies of specific systems catalyzed by titanium hydrides,^{2–5} over the last 10 years, much needed attention has been paid to the fundamental chemistry of simple titanium hydride systems.

Recently Andrews et al. carried out low-temperature matrix isolation studies on the reaction between laser-ablated titanium atoms and hydrogen.⁶ Previously to this Margrave, Xiao, and Hauge carried out similar experiments in which they studied the reaction of titanium atoms, produced by the vaporization of a titanium filament, with hydrogen.⁷ These two studies between them produced the first reported spectra of the molecules TiH, TiH₂, TiH₃, and TiH₄.

Bauschlicher has carried out a series of *ab initio* calculations on TiH including benchmark full CI calculations.⁸ *Ab initio* calculations carried out on TiH₂ have shown its ground state to be a triplet with bent geometry.⁹ Studies on H₂- - -TiH₂ and TiH₄¹⁰ have attempted to clarify peak assignments made in

Margrave's experimental work.⁷ Also, an *ab initio* study done in this laboratory¹¹ investigated the dimerization of TiH₄ and concluded that TiH₄ dimers could have been observed in the matrix isolation studies.^{6,7} Most recently a study carried out on singlet closed-shell Ti₂H₆¹² finds two C_{3v} triple bridged structures: one with an eclipsed conformation and the other staggered. No Ti–Ti bonding interaction was found in these isomers despite short Ti–Ti separations. At their best level of theory Garcia and Ugalde found the structures to be ~20 kcal/mol lower in energy than 2TiH₃. However, in this paper, we will show that the single-determinant reference wave function used in their study provides an inadequate description of the Ti₂H₆ system. Consequently, the Ti₂H₆ potential energy surfaces need to be reexamined.

In this work, we have carried out an extensive study of the potential energy surfaces of the lowest singlet and triplet states of Ti₂H₆, in part to investigate the diradical character of this system. We have considered both singlet and triplet states of double, triple, and quadruple hydrogen bridged structures. This study also addresses the energy of Ti₂H₆ relative to two separated TiH₃ monomers. Obviously this has some bearing on the experimental work of Andrews et al.,⁶ who claim to have observed TiH₃, as dimers could be present in their matrix isolation experiments. Calculations of the infrared frequencies of TiH₃ and Ti₂H₆ are reported for comparison with experiment. We also consider the thermodynamics of reactions R1 and R2.



The molecule H₂Ti(μ -H)₂TiH₂ is an important prototype as it can serve as the simplest model for homodinuclear titanium-(III) systems. There are numerous examples of such systems

(1) Toogood, G. E.; Wallbridge, M. G. H. *Adv. Inorg. Chem. Radiochem.* **1982**, *25*, 267.

(2) Bode, B.; Day, P. N.; Gordon, M. S. *J. Am. Chem. Soc.* **1998**, *120*, 1552.

(3) Kawamura-Kuribayashi, H.; Koga, N.; Morokuma, K. *J. Am. Chem. Soc.* **1992**, *114*, 2359.

(4) Gauvin, F.; Britten, J.; Samuel, E.; Harrod, J. F. *J. Am. Chem. Soc.* **1992**, *114*, 1489.

(5) Jolly, C. A.; Marynick, D. S. *J. Am. Chem. Soc.* **1989**, *111*, 7968.

(6) Chertihin, G. V.; Andrews, L. *J. Am. Chem. Soc.* **1994**, *116*, 8322.

(7) Xiao, Z. L.; Hauge, R. H.; Margrave, J. L. *Phys. Chem.* **1991**, *95*, 2696.

(8) Bauschlicher, C. W. *J. Phys. Chem.* **1988**, *92*, 3020.

(9) (a) Fujii, T. S.; Iwata, S. *Chem. Phys. Lett.* **1996**, *251*, 150. (b) Kudo, T.; Gordon, M. S. *J. Chem. Phys.* **1995**, *102*, 6806.

(10) (a) Ma, B.; Collins, C. L.; Schaefer, H. F. *J. Am. Chem. Soc.* **1996**, *118*, 870. (b) Schaefer, H. F. *J. Chem. Phys.* **1992**, *96*, 6857.

(11) Webb, S. P.; Gordon, M. S. *J. Am. Chem. Soc.* **1995**, *117*, 7197.

(12) Garcia, A.; Ugalde, J. M. *J. Phys. Chem.* **1996**, *100*, 12277.

in the literature. The compound $rac\text{-}\{[C_2H_4(\eta^5\text{-tetrahydroindenyl})_2]Ti^{III}(\mu\text{-H})\}_2^{13}$ contains a Ti_2H_2 unit with the two hydrogens bridging to form a flat ring. It is the first structurally characterized titanocene(III) hydride derivative without a supporting organic bridge and is found to be antiferromagnetic. The titanocene dimer $[(\eta^5\text{-}C_5H_5)Ti(\mu\text{-H})]_2(\mu\text{-}\eta^5\text{-}\eta^5\text{-}C_{10}H_8)$ has also been shown to have two bridging hydrogens between its two titanium(III) centers, but in contrast to the compound just discussed, the Ti_2H_2 unit forms a buckled ring with folding along the H - -H axis and there is a carbon-carbon linkage between titanocene units.¹⁴ It is found to be diamagnetic at ambient temperature, which suggests either a Ti-Ti bond and/or a substantial singlet-triplet energy gap as the Ti(III) d electrons must be paired or singlet coupled; however, due to lack of detailed magnetic susceptibility measurements as a function of temperature, this has not been established definitively and is the subject of ongoing calculations in this laboratory. The hydroxy derivative of the titanocene dimer¹⁵ was found to be weakly paramagnetic, suggesting diradical character, although the authors were hesitant to rule out Ti-Ti bonding. Other studies include those on $[Cp_2Ti(\mu\text{-X})]_2$, where X = F, Cl, Br, and I.^{16,17} They find unpaired electrons exhibiting antiferromagnetic behavior with strengths in the order Br > Cl ~ I > F, suggesting dependence on more than just Ti-Ti distance. Two more recent experimental studies^{18,19} also demonstrate the sensitivity of the magnetic properties associated with these homodinuclear titanium(III) compounds to the bridging species. Samuel et al. find that the compounds $[Cp_2Ti(\mu\text{-OCH}_3)]_2$ and $[Cp_2Ti(\mu\text{-OC}_2H_5)]_2$ are paramagnetic dimers exhibiting weak antiferromagnetic behavior suggesting singlet coupling of unpaired electrons. However, Dick et al. find the compounds $[Cp_2Ti(\mu\text{-PMe}_2)]_2$ and $[Cp_2Ti(\mu\text{-PEt}_2)]_2$ to be diamagnetic and strongly antiferromagnetic. They suggest either through-ligand coupling of the unpaired Ti electrons or a "super-long" σ -type Ti-Ti bond of the type proposed to be present in certain homodinuclear zirconium systems by Rohmer and Bénard.²⁰ The latter appears unlikely considering the Ti-Ti separation of ~3.7 Å. Another example is the complex $[Cp_2Ti(\mu\text{-O})]_2$, which is paramagnetic and weakly ferromagnetic.²¹ This is the only ferromagnetic homodinuclear Ti(III) compound known.

It is clear then that the bonding and magnetic properties of these molecules arise from complex interactions between the two metal centers and between the metal centers and bridging (and possibly terminal) ligands. With the current and constantly increasing scope of *ab initio* calculations, it seems reasonable to expect helpful and reliable contributions from "first principles" theory in this area soon. However, establishing adequate levels of theory to describe simple dinuclear titanium(III) systems is vital before approaching the complex systems just described. This is best done by first considering the prototypical $H_2Ti(\mu\text{-H})_2TiH_2$ system. It is relatively straightforward (relative

to experiment) to establish the nature of Ti-Ti interactions using theoretical techniques such as the calculation of natural orbital occupations of MCSCF wave functions. In subsequent studies, one could then monitor directly the effect of, for example, terminal cyclopentadienyl ligands and various bridging ligands on the Ti-Ti interaction in homodinuclear titanium(III) systems by comparison to the "baseline" $H_2Ti(\mu\text{-H})_2TiH_2$ analysis.

The ability to predict magnetic properties of dinuclear complexes is an important goal in the area of molecular materials.²² The use of *ab initio* calculations in this area has until recently been rather limited. Accurate determination of multiplet splitting energies requires the inclusion of nondynamic and dynamic correlation effects.^{23,24} The relative simplicity of $H_2Ti(\mu\text{-H})_2TiH_2$ enables us to make a reliable determination of its singlet-triplet splitting energy.

II. Computational Details

(a) Basis Set. For titanium, we employed a triple- ζ with polarization (14s11p6d/10s8p3d) basis set. This consists of Wachter's basis set²⁵ with two additional sets of p functions and a set of diffuse d functions.²⁷ For hydrogen Dunning's (5s1p/3s1p) basis set²⁸ was used. Collectively this basis set is referred to as TZVP and was used in all geometry optimizations. F functions were added to the titanium basis with an exponent of 0.4¹¹ for single-point energies; this basis set is referred to as TZVP(f). For a final test of basis set convergence, selected single-point energies were carried out with the titanium TZVP basis plus one set of f ($\alpha = 0.591$) and g ($\alpha = 0.390$) functions and a set of diffuse s ($\alpha = 0.035$), p ($\alpha = 0.239$), and d ($\alpha = 0.0207$) functions. Exponents used here are optimized for correlated titanium atoms and are due to Glezakou and Gordon.²⁹

(b) Wave Functions. We now discuss the wave functions needed to adequately describe a reference state for the Ti_2H_6 isomers we consider in this paper (see Figure 1). Garcia and Ugalde carried out the only previous calculations on Ti_2H_6 .¹² They reported only singlet C_{3v} triple bridged structures and used closed-shell single-determinant reference wave functions. However, careful consideration of the orbitals and electrons reveals the inadequacy of such a single-configuration description. These C_{3v} isomers require consideration of three orbitals (a_1 , e_s , and e_y) for occupation of the two highest energy electrons, due to the near degeneracy of the orbitals. Several electronic states correspond to the distribution of two electrons in this orbital space: two 1A_1 states, four 1E states, one 3A_2 state, and two 3E states (see Figure 2a,b). These group theoretical considerations suggest the need for a multiconfigurational (MC) SCF description of those states.

Preliminary fully optimized reaction space (FORS)-MCSCF³⁰ (also called CASSCF³¹) calculations illustrate considerable mixing between the $(a_1)^2(e_s)^0(e_y)^0$ and $((a_1)^0(e_s)^2(e_y)^0 + (a_1)^0(e_s)^0(e_y)^2)$ configurations in the 1A_1 ground state: a natural orbital analysis of the eclipsed isomer wave function shows 1.51 electrons in the a_1 orbital and 0.24 electrons in each of the degenerate e orbitals. This qualitatively correct

(22) (a) Kahn, O. *Angew. Chem., Int. Ed. Engl.* **1985**, *24*, 834. (b) Kahn, O. *Molecular Magnetism*; VCH: New York, 1993; Chapters 6-9.

(23) Mödl, M.; Povill, A.; Rubio, J.; Illas, F. *J. Phys. Chem. A* **1997**, *101*, 1526.

(24) Castell, O.; Caballol, R.; García, V. M.; Handrick, K. *Inorg. Chem.* **1996**, *35*, 1609.

(25) Wachters, A. J. H. *J. Chem. Phys.* **1970**, *52*, 1033.

(26) Hood, D. M.; Pitzer, R. M.; Schaefer, H. F. *J. Chem. Phys.* **1979**, *71*, 705.

(27) Rappe, A. K.; Smedley, T. A.; Goddard, W. A. *J. Phys. Chem.* **1981**, *85*, 2607.

(28) Dunning, T. H.; Hay, P. J. In *Methods of Electronic Structure Theory*; Schaefer, H. F., III, Ed.; Plenum Press: New York, 1977; pp 1-27.

(29) Glezakou, V.-A.; Gordon, M. S. *J. Phys. Chem.* **1997**, *101*, 8714.

(30) (a) Sunberg, K. R.; Ruedenberg, K. In *Quantum Science*; Calais, J. L., Gosinski, O., Linderberg, J., Ohm, Y., Eds.; Plenum: New York, 1976; p 505. (b) Cheung, L. M.; Sunberg, K. R.; Ruedenberg, K. *Int. J. Quantum Chem.* **1979**, *16*, 1103. (c) Ruedenberg, K.; Schmidt, M.; Gilbert, M. M.; Elbert, S. T. *Chem. Phys.* **1982**, *71*, 41.

(31) Roos, B. O.; Taylor, P.; Siegbahn, P. E. M. *Chem. Phys.* **1980**, *48*, 157.

(13) Xin, S.; Harrod, J. F.; Samuel, E. *J. Am. Chem. Soc.* **1994**, *116*, 11562.

(14) (a) Troyanov, S. I.; Antropiusová, H.; Mach, K. *J. Organomet. Chem.* **1992**, *427*, 49. (b) Davidson, A.; Wreford, S. S. *J. Am. Chem. Soc.* **1974**, *96*, 3017. (c) Brintzinger, H. H.; Bercaw, J. E. *J. Am. Chem. Soc.* **1970**, *92*, 6182.

(15) Guggenberger, L. J.; Tebbe, F. N. *J. Am. Chem. Soc.* **1976**, *98*, 4137.

(16) Coutts, R. S. P.; Wailes, P. C.; Martin, R. L. *J. Organomet. Chem.* **1973**, *47*, 375.

(17) Jungst, R.; Sekutowski, D.; Davis, J.; Luly, M.; Stucky, G. *Inorg. Chem.* **1977**, *16*, 1645.

(18) Samuel, E.; Harrod, J. F.; Gourier, D.; Dromzee, Y.; Robert, F.; Jeannin, Y. *Inorg. Chem.* **1992**, *31*, 3252.

(19) Dick, D. G.; Stephan, D. W. *Can. J. Chem.* **1991**, *69*, 1146.

(20) Rohmer, M.; Bénard, M. *Organometallics* **1991**, *10*, 157.

(21) Lukens, W. W.; Andersén, R. A. *Inorg. Chem.* **1995**, *34*, 3440.

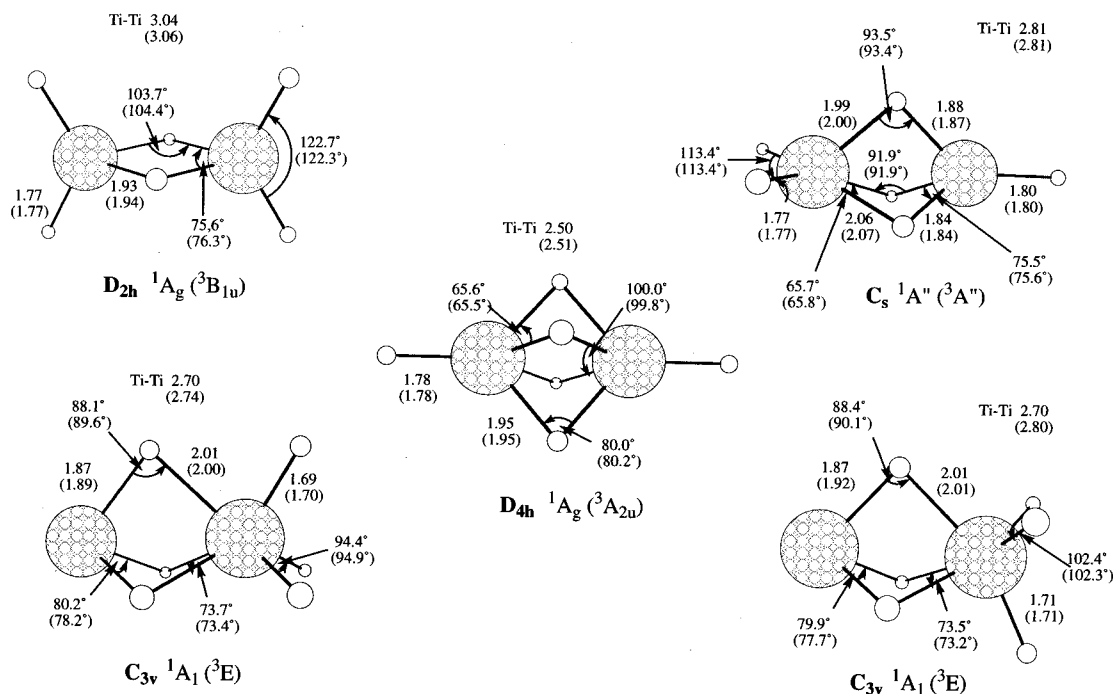


Figure 1. MCSCF/TZVP singlet and ROHF/TZVP triplet local minima on the two lowest potential energy surfaces of Ti_2H_6 . Bond lengths are in angstroms. Brackets signify triplet geometry.

description of the 1A_1 ground state (taking the eclipsed isomer as an example) is 13.6 kcal lower in energy than the 1A_1 state described with the RHF closed-shell wave function $(a_1)^2(e_x)^0(e_y)^0$. Therefore, the two-electron, three-orbital MCSCF wave function is the *simplest qualitatively correct wave function* for the 1A_1 states. It is the reference wave function used in subsequent perturbation calculations which correct for dynamic electron correlation (that is, the inherent deficiency of the wave function introduced by the orbital approximation) in the 1A_1 states. Tests for possible Jahn–Teller distortions to lower symmetries suggest that such distortions are negligible (see the Appendix).

It is formally possible for all four of the 1E configurations to mix; however, a preliminary FORS-MCSCF calculation suggests that a subset of the 1E configurations are dominant in each excited 1E state. The first two degenerate excited 1E states are dominated by the configurations $(a_1)^1(e_x)^1(e_y)^0$ and $(a_1)^1(e_x)^0(e_y)^1$ (all other CI coefficients are less than 0.025). Therefore, a “state-averaged” restricted open-shell Hartree–Fock (ROHF) wave function was constructed by assigning equal weights to these two dominant configurations. This single-configuration ROHF wave function is then used to predict the staggered and eclipsed geometries. It also serves as the reference for perturbation corrections on the averaged 1E excited state.

The C_{3v} 1E state is considerably higher in energy than the C_{3v} 1A_1 state. This is also the case when dynamic electron correlation is accounted for. Since our primary interest is in the nature of the ground-state singlet potential energy surface, this higher state is not considered further. The same is true for the third and fourth 1E excited states, whose dominant configurations are shown in Figure 2a.

The two degenerate 3E components $((a_1)^1(e_x)^1(e_y)^0)$ and $(a_1)^1(e_x)^0(e_y)^1$ are described by a state-averaged wave function. This state-averaged 3E state is lower in energy than the 3A_2 state (see Figure 2b). The 3E and 3A_2 states can both be described qualitatively correctly with a single-determinant ROHF wave function. With inclusion of dynamic electron correlation, the 3E state is considerably lower in energy than the 3A_2 state. Since 3E is the lowest energy triplet, the 3A_2 state is not considered further.

Test calculations on the *lowest energy* singlet states for other Ti_2H_6 isomers (D_{2h} , C_s , and D_{4h}) show that a correct reference wave function requires the inclusion of only two orbitals and the two highest energy electrons in the active space. This is discussed in the next subsection.

(c) Methods. For Ti_2H_6 triplets and the TiH_3 doublet, geometry optimizations were performed at the ROHF level of theory. For singlets, preliminary calculations were carried out at the RHF level.

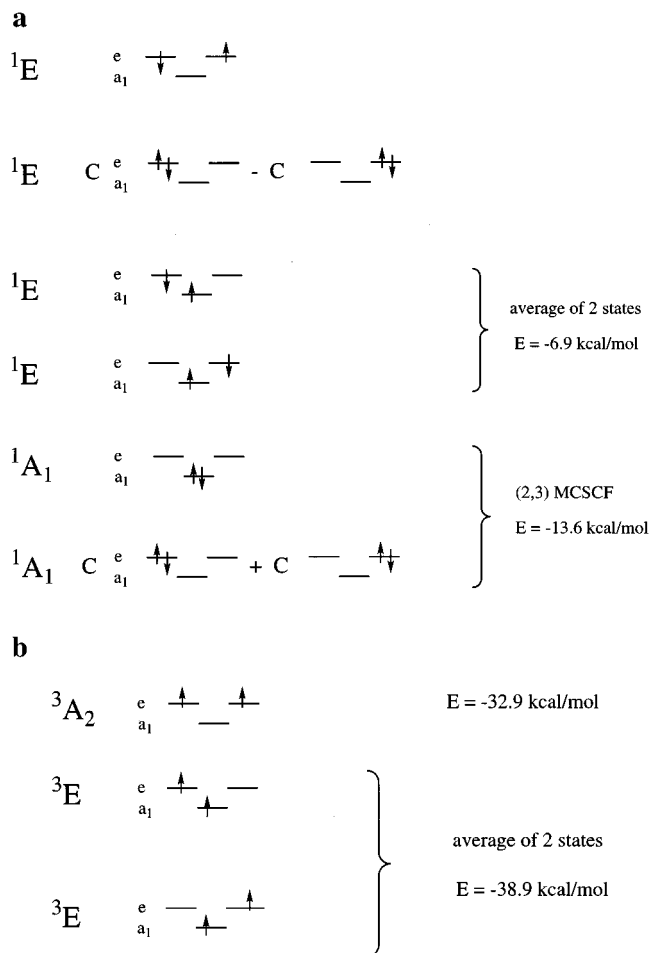


Figure 2. Possible (a) singlet and (b) triplet states for C_{3v} isomers. Energies given are for the eclipsed isomer and are relative to the closed-shell RHF energy with double occupation of the a_1 orbital.

After convergence of the RHF wave function, modified virtual orbitals (MVOs) were used as a starting point for two-configuration (TCSCF)

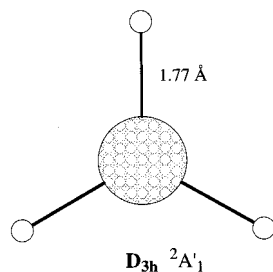


Figure 3. ROHF/TZVP-optimized minimum energy structure of TiH_3 .

geometry optimizations, and two electrons in three orbitals, FORS-MCSCF geometry optimizations where necessary (e.g., $C_{3v} \ ^1A_1$). The $^1A''$ state of the C_s structure was found to be lower in energy than the $^1A'$ state, so geometries reported for this singlet were obtained from an ROHF calculation. TCSCF wave functions frequently overestimate diradical character. To ensure that the high diradical character found in the Ti_2H_6 isomers in this study is not an artifact of the small active spaces, a FORS-MCSCF/TZVP geometry optimization with 12 electrons in 13 orbitals on the D_{2h} isomer was carried out. This active space is at the limit of our capabilities and includes all but two of the valence electrons in Ti_2H_6 . The seven virtual orbitals included in the active space correspond to d-orbital interactions of various orientations. The natural orbital analysis of the resulting wave function is virtually identical to that of the TCSCF wave function. The occupation numbers of the Ti–Ti σ and σ^* natural orbitals in the (12,13) wave function are 1.15 and 0.85 electrons, respectively, compared with 1.11 and 0.89 for the TCSCF calculation. All other occupation numbers are ~ 2.0 or 0.0 in the (12,13) calculation. FORS-MCSCF/TZVP calculations with a (2,10) active space which includes all possible d-orbital orientations also confirm the same diradical character and adequacy of the TCSCF wave function.

Stationary points were characterized by calculating and diagonalizing the energy second-derivative matrix (Hessian). A positive definite Hessian (no negative eigenvalues) indicates a minimum on the potential energy surface.

Dynamic electron correlation effects were included by carrying out RMP2³² single-point energy calculations at ROHF geometries for C_s , D_{2h} , and D_{4h} triplets and multiconfigurational quasidegenerate second-order perturbation theory calculations (MCQDPT)³³ at the ROHF geometries for the $C_{3v} \ ^3E$ and $C_s \ ^1A''$ states, TCSCF geometries for D_{2h} and D_{4h} singlets, and the two-electron, three-orbital FORS-MCSCF geometry for the $C_{3v} \ ^1A_1$ state (note: any future reference to MCSCF will imply FORS-MCSCF). For energetics these single-point energy calculations were repeated with the TZVP(f) basis set. For energies relative to 2TiH_3 consistent methodology was used, i.e. the dimerization energy was calculated with both energies from RMP2 or both energies from MCQDPT. Additional single-point energy calculations on the C_s , D_{2h} , and D_{4h} singlets and triplets were carried out using the largest basis set TZVP(f,g) as a test of basis set convergence.

All calculations were done using the electronic structure code GAMESS.³⁴

III. Results and Discussion

TiH_3 . A D_{3h} structure ($^2A'_1$ state) was found to be the lowest energy minimum on the TiH_3 potential energy surface and is shown in Figure 3. Total energies are available as Supporting Information (Table S1).

Ti_2H_6 . Multiple minima were found on both the triplet and singlet potential energy surfaces of Ti_2H_6 . Geometries are

(32) (a) Knowles, P. J.; Andrews, J. S.; Amos, R. D.; Handy, N. C.; Pople, J. A. *Chem. Phys. Lett.* **1991**, *186*, 130. (b) Lauderdale, W. J.; Stanton, J. F.; Gauss, J.; Watts, J. D.; Bartlett, R. J. **1991**, *187*, 21.

(33) (a) Nakano, H. *J. Chem. Phys.* **1993**, *99*, 7983. (b) Nakano, H. *Chem. Phys. Lett.* **1993**, *207*, 372.

(34) Schmidt, M. W.; Baldridge, K. K.; Boatz, J. A.; Jensen, J. H.; Koseki, S.; Matsunaga, N.; Gordon, M. S.; Ngugen, K. A.; Su, S.; Windus, T. L.; Elbert, S. T.; Montgomery, J.; Dupuis, M. *J. Comput. Chem.* **1993**, *14*, 1347.

shown in Figure 1. Energies relative to $^2A'_1 \ 2\text{TiH}_3$ (at 0 K) and zero-point energy differences are shown in Table 1. For the most part energetics discussed are those on the classical potential energy surface (no zero-point energy correction included). Molecular orbital plots along with occupation numbers are shown in Figure 4a,b.

(a) Molecular and Electronic Structure, and Energetics. All the structures found in this study of Ti_2H_6 (see Figure 1) involve bridging hydrogens between the two titanium(III) centers. The presence of bridging hydrogens is not particularly surprising and may be attributed to the electron deficiency of the two titaniums and their desire for high coordination numbers.¹¹ The double hydrogen bridged ($\mu\text{-H}$)₂ minima (singlet and triplet) closely resemble the structure of diborane. These D_{2h} structures may be thought of as simple prototypes in which the two titaniums and the bridging ligands are arranged in a fashion similar to that in more complex homodinuclear titanium(III) compounds such as titanocene dimer.¹⁴ From this perspective, the bonding and energetic characteristics of the D_{2h} structure, such as diradical character and singlet–triplet splitting (see sections IIIc and III d), may be thought of as a reference with which to compare these more complex systems. It does not appear that any triple ($\mu\text{-H}$)₃ or quadruple ($\mu\text{-H}$)₄ hydrogen bridged dititanium(III) compounds are experimentally known. Homodinuclear transition metal compounds containing Fe and Re with three and four bridging hydrogens, respectively, are known experimentally. Examples are $[\text{Fe}_2(\mu\text{-H})_3(\text{P}_3)]^+$ ³⁵ and $\text{Re}_2(\mu\text{-H})_4 \text{H}_4(\text{PEt}_2\text{Ph})_4$.³⁶ So, the remaining ($\mu\text{-H}$)₃ and ($\mu\text{-H}$)₄ isomers are not yet useful as prototypes, but are highly relevant to the low-temperature matrix isolation studies of Margrave⁷ and Andrews⁶ (see section IIIb).

The D_{2h} , C_s , and D_{4h} ground-state minima either exhibit a high degree of diradical character (D_{2h} and D_{4h} singlets) or are by definition diradicals (triplets and $C_s \ ^1A''$). A natural orbital analysis of the singlet TCSCF/TZVP wave functions (see Figure 4a) shows occupancies of 1.11 and 0.89 electrons for the σ and σ^* orbitals, respectively, in the D_{2h} singlet minimum and 1.09 and 0.91 electrons for π and π^* , respectively, in the D_{4h} singlet minimum. These occupation numbers indicate high diradical character with a very small bonding interaction in these two singlets. Another indication of the D_{2h} and D_{4h} singlet diradical character is the near degeneracy of the TCSCF singlet and the ROHF triplet energies for these structures (Table 1). Of course, if one assumes identical geometries, a pure diradical singlet when excluding dynamic electron correlation will necessarily be higher in energy than a triplet, due to the intrinsic correlation of the same spin electrons in the triplet. This is in fact the case for the C_s isomer, for which the singlet is purely diradical: the triplet is lower in energy by 0.5 kcal/mol. The D_{2h} and D_{4h} singlets are 0.5 and 0.6 kcal/mol lower in energy than their triplet counterparts, respectively. This reinforces what was suggested by the natural orbital analysis (see Figure 4a): there is a very weak bonding interaction in these two singlets. At our best level of theory for these isomers, which includes f and g functions on Ti and dynamic electron correlation through second-order perturbation theory (MCQDPT/TZVP(f,g)), we can draw similar conclusions: the C_s singlet and triplet isomers are essentially degenerate with the triplet only 0.3 kcal/mol lower in energy than the singlet, whereas the D_{2h} and D_{4h} singlets are lower in energy than their triplet counterparts by 1.3 and 1.4 kcal/mol, respectively, again suggesting weak bonding interac-

(35) Dapporto, P.; Fallani, G.; Midollini, L.; Sacconi, L. *J. Am. Chem. Soc.* **1973**, *95*, 2023.

(36) Bau, R.; Carroll, W. E.; Teller, R. G.; Koetzle, T. F. *J. Am. Chem. Soc.* **1977**, *99*, 3872.

Table 1. All Energies Relative to 2TiH_3 D_{3h} ${}^2A'_1$ Monomer Energy in kcal/mol ($E = E(\text{Ti}_2\text{H}_6) - E(2\text{TiH}_3)$)

point group	MCSCF active space	state	singlet					triplet					
			TZVP			TZVP(f)	TZVP(f,g)	TZVP			TZVP(f)	TZVP(f,g)	
			MCSCF	ZPE ^a	MCQDPT	MCQDPT	MCQDPT	state	ROHF	ZPE ^a	RMP2	RMP2	RMP2
C_s	not applicable, ROHF used	${}^1A''$	-41.0	4.4	-55.0	-55.2	-56.1	${}^3A''$	-41.5	4.4	-53.2	-55.5	-56.4
D_{2h}	(2,2)	1A_g	-42.9	3.8	-49.6	-51.2	-51.6	${}^3B_{1u}$	-42.4	3.7	-48.5	-50.0	-50.3
D_{4h}	(2,2)	1A_g	-22.2	5.1	-45.2	-50.5	-51.5	${}^3A_{2u}$	-21.8	5.1	-44.0	-49.1	-50.1
C_{3v}	eclipsed	1A_1	13.3	5.2	-27.1	-31.2	—	3E	-11.9	5.2	-45.0 ^b	-48.3 ^b	—
	staggered	1A_1	13.3	4.6	-22.4	-26.3	—	3E	-11.8	4.7	-40.2 ^b	-43.2 ^b	—

^aZero-point energies were calculated at the MCSCF/TZVP and ROHF/TZVP levels and were scaled by 0.948 (see section IIIb for details of scaling factor). ^bNote that dynamic correlation effects in the C_{3v} 3E structures were calculated using the MCQDPT method.

tions. The singlet–triplet energy gap for the D_{2h} isomer will be discussed in more detail in section III d, where we consider magnetic properties.

The diradical nature of these isomers cannot be attributed to large Ti–Ti separations. One can clearly see from Figure 1 that the Ti–Ti separations (3.04, 2.81, and 2.50 Å for the D_{2h} , C_s , and D_{4h} singlets, respectively) are close to or well within a separation one might normally associate with a titanium bond based on the titanium atomic radius of 1.47 Å.³⁷ For the C_s , D_{4h} , and C_{3v} isomers, inspection of the orbitals is sufficient to suggest why there is no Ti–Ti bond formation. Figure 4a shows the relevant d orbitals of the C_s structure. Their orientation presumably reflects a minimization of unfavorable interactions with bridging and terminal hydrogens. The result is d orbital orientations in which no overlap or interaction can be expected and so single occupation of two orthogonal orbitals (one on each titanium) is energetically favored. For the D_{4h} structure Figure 4a shows the d orbitals to be in a π arrangement. It appears here that even the short Ti–Ti separation of 2.50 Å is too long for effective π orbital overlap. The C_{3v} structures show a coordination number of 6 on one Ti and only 3 on the other, making one titanium less saturated than the other. The two electrons prefer to associate with the less saturated Ti in a nonbonding lone pair arrangement (Figure 4b).

For the D_{2h} singlet, mere inspection of the orbitals (Figure 4a) does not make it clear at all why there is no Ti–Ti bond to speak of. Here the orbitals are in an ideal arrangement for the formation of a σ bond yet there is only a weak bonding interaction. An explanation of the lack of a strong bonding interaction between the two titaniums in the D_{2h} structure will be suggested in section III c).

The Ti–H bond length behavior (see Figure 1) is similar to that seen in the related Ti_2H_8 isomers.¹¹ The terminal Ti–H bond lengths are between 1.7 and 1.8 Å, within the range of Ti–H bond lengths found in TiH_4 (1.70 Å) and TiH_3 (1.77 Å) at equivalent levels of theory (same basis set, no dynamic correlation). Bridging Ti–H bonds are, as expected, longer than terminal Ti–H bonds by up to ~ 0.2 Å.

Dynamic electron correlation is included through single-point energies using second-order perturbation theory. At this level of theory, the $(\mu\text{-H})_3$ C_s structures (singlet and triplet) are clearly the lowest in energy (Table 1). So, as has been shown previously,¹¹ dynamic electron correlation preferentially favors isomers with more than two bridging hydrogens. The D_{4h} isomers with the TZVP basis set are stabilized by 23.0 and 22.2 kcal/mol for the singlet and triplet, respectively, and the C_{3v} isomers are stabilized by 40.4 and 33.1 kcal/mol for the singlet and triplet eclipsed structure. Dynamic electron correlation

narrows the spread of isomer energies considerably. Another effect of electron correlation is to lower the energies of the eclipsed C_{3v} isomers with respect to the staggered isomers by between 4 and 5 kcal/mol. This was also noted by Garcia and Ugalde.¹² With the inclusion of dynamic electron correlation all ground-state isomers (including C_{3v} singlets) are lower in energy than the separated monomers 2TiH_3 . At the best level of theory, including zero-point energy corrections (calculated using MCSCF/TZVP and ROHF/TZVP) at 0 K, the TiH_3 dimer is thermodynamically favored over the monomer by up to 52.0 kcal/mol (ΔH for C_s ${}^3A''$ isomer). Previous work suggests no kinetic barrier to the dimerization of simple titanium hydrides;¹¹ therefore, one might expect rapid dimerization whenever two TiH_3 molecules approach each other.

Inclusion of Ti f functions appears to be necessary for a reliable description of the whole range of Ti_2H_6 isomers. Their presence has a noticeable effect on the D_{4h} and C_{3v} structures, lowering their energies (relative to 2TiH_3) by 5.3, 5.1 (D_{4h} singlet and triplet, respectively), 4.0, and 3.0 kcal/mol (C_{3v} singlet and triplet, respectively) at the correlated level. Increasing the basis set further to TZVP(f,g) makes little difference (0.3–1.0 kcal/mol) to the predicted dimerization energies, so the TZVP(f) basis provides a good description of the entire range of isomers.

(b) Calculated IR Frequencies. Vibrational frequencies were calculated at the MCSCF/ROHF TZVP level for all minima. The C_s ${}^3A''$, D_{2h} 1A_g , D_{4h} 1A_g , and staggered C_{3v} 3E minima were chosen for comparison with experimental spectra.

The matrix isolation experiments of Margrave et al.⁷ and Andrews et al.⁶ produced the first spectra of simple titanium hydrides. The spectra are very complex; imperfect isolation presumably results in the coexistence of many different titanium hydride species. It has already been shown that the existence of Ti_2H_8 in these experiments is possible.¹¹ We now examine the likelihood of the presence of Ti_2H_6 , having shown this species to be considerably lower in energy than 2TiH_3 . The assigned experimental Ti–H stretch frequency for TiH_3 is 1580.6 cm^{-1} ; the calculated ROHF/TZVP stretch frequency is 1668.0 cm^{-1} . The calculated stretch frequency, then, may be scaled to the experimental one by a factor of 0.948. All frequencies discussed here are therefore scaled by this factor. Calculated IR frequencies, their corresponding intensities, and experimental frequencies are shown in Table 2.

The spectrum produced by Andrews et al. has better resolution than that produced by the Margrave group; therefore, comparisons are made mainly with Andrews' data. Broad absorptions corresponding to bridge stretches and bends are characteristic of hydrogen bridged titanium compounds. Two such broad features can be seen in the experimental spectra.⁶ The first lies between ~ 1440 and $\sim 1560\text{ cm}^{-1}$ and is fairly well resolved;

(37) Clark, R. J. H. *The Chemistry of Titanium and Vanadium*; Elsevier: Amsterdam, 1968; p 6.

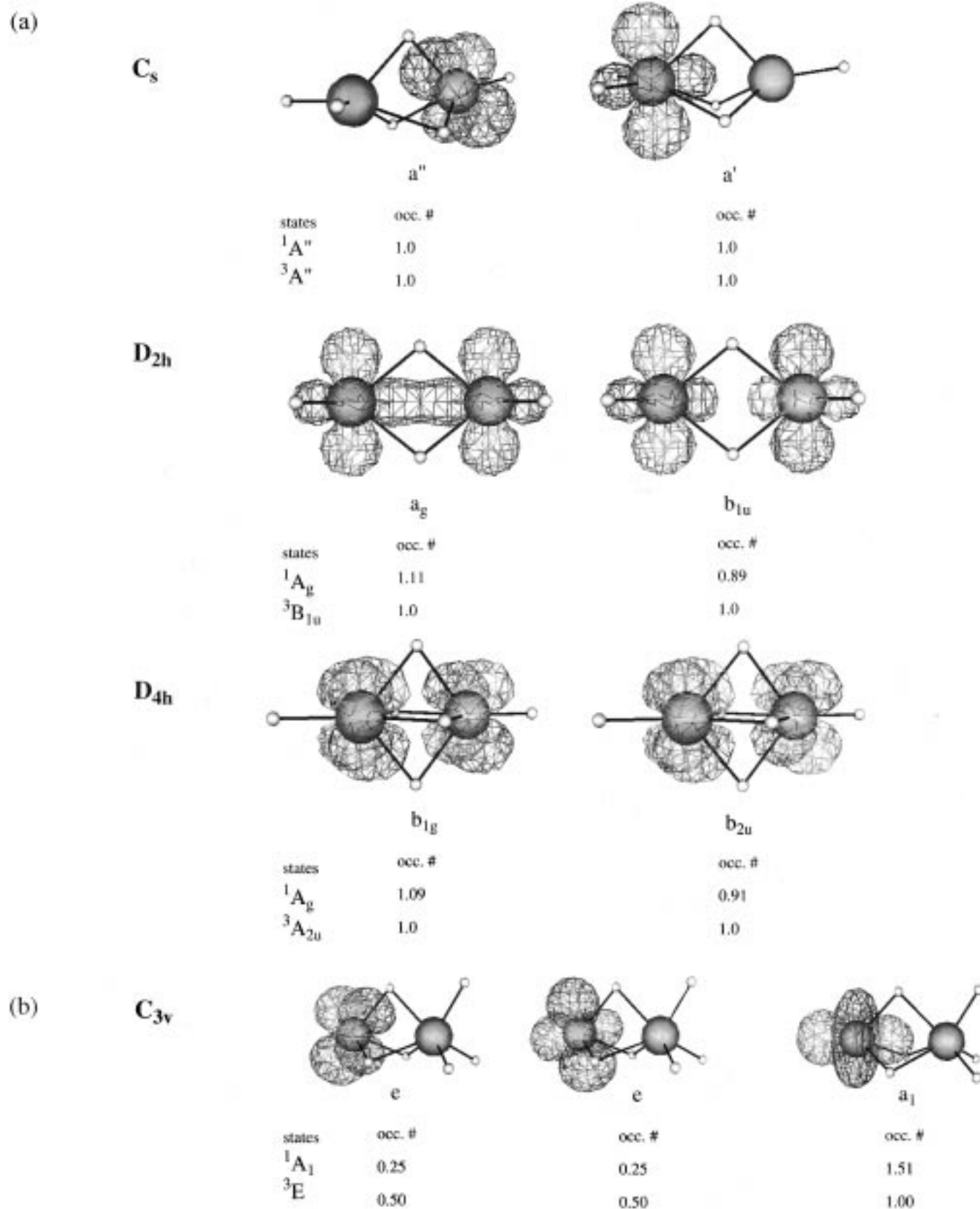


Figure 4. (a) Three-dimensional plots of the two HOMOs in the C_s , D_{2h} and D_{4h} Ti_2H_6 isomers. For the D_{2h} and D_{4h} singlets, these orbitals constitute the active orbitals used in the TCSCF calculations. Occupation numbers shown for the D_{2h} and D_{4h} isomers are from a natural orbital analysis. (b) Three-dimensional plots of the three active molecular orbitals in the 1A_1 and 3E C_{3v} eclipsed isomers. Singlet occupation numbers are from a natural orbital analysis. Singlet and triplet state orbitals are qualitatively the same; therefore, only one set is shown. The orbital contour value used is $0.04 \text{ bohr}^{3/2}$.

the second lies between ~ 1150 and $\sim 1340 \text{ cm}^{-1}$ with only partial resolution. The most intense calculated frequency for

the C_s $^1A''$ species is 1475.9 cm^{-1} ; this is a bridge stretch and is close to the resolved experimental peak at 1485.2 cm^{-1} .

Table 2. Calculated Harmonic Vibrational Frequencies for Selected Ti_2H_6 Isomers^a

vibration	intensity (km mol^{-1})	frequency (cm^{-1})	scaled frequency (cm^{-1})	exptl frequency (cm^{-1}) ^b	exptl assign.
C_s ($^1A''$)					
H _t bend	296.2	625.7	593.0	500 (broad)	Ti _x H _y
H _{br} bend	402.3	744.2	705.2		
H _{br} bend	376.1	831.0	787.5		
H _{br} bend	751.7	1204.3	1141.3		
Ti–H _{br} str.	398.0	1375.7	1303.7	1305	
Ti–H _{br} str.	1829.6	1557.4	1475.9	1485.2	Ti _x H _y
Ti–H _t str.	921.2	1656.8	1570.1	1570	
Ti–H _t str.	356.6	1706.6	1617.2	1632	Ti _x H _y
D_{2h} (1A_g)					
H _t bend	376.6	574.8	544.7	500 (broad)	Ti _x H _y
H _{br} bend	175.4	744.6	705.6		
Ti–H _{br} str.	663.8	1128.5	1069.4		
Ti–H _{br} str.	2249.7	1412.9	1338.9	1330	
Ti–H _t str.	2040.1	1679.5	1591.5	1590	
Ti–H _t str.	328.7	1749.2	1657.6	1656.7	TiH ₄
D_{4h} (1A_g)					
H _{br} bend	213.8 (×2)	943.9	894.4		
Ti–H _{br} str.	2360.8	1254.6	1188.9	1200	
Ti–H _{br} str.	898.8 (×2)	1290.7	1223.1	1225	}Ti _x H _y
Ti–H _t str.	1437.5	1685.0	1596.8	1590	
C_{3v} (3E)					
H _{br} bend	136.9 (×2)	808.3	766.0		
H _{br} bend	411.1	892.5	845.7		
Ti–H _{br} str.	1659.4	1139.3	1079.6		
Ti–H _{br} str.	313.1	1485.2	1407.4	1422.7	TiH(H ₂)
Ti–H _t str.	711.6 (×2)	1742.3	1651.0	1640.5	Ti _x H _y

^a A scaling factor of 0.948 was used. Only calculated frequencies with an intensity greater than 100 km/mol are reported. H_t = terminal hydrogen; H_{br} = bridging hydrogen.

Andrews assigns this peak to the species Ti_xH_y. A number of the calculated frequencies lie within the broad 1150–1340 cm^{-1} experimental feature (note that Andrews assigns this broad feature which is centered on 1250 cm^{-1} to Ti_xH_y; see spectra for details⁶). The most intense of these calculated frequencies is for the D_{4h} 1A_g species and appears at 1188.9 cm^{-1} ; this corresponds to an experimental peak seen at 1200 cm^{-1} . A second calculated frequency for D_{4h} 1A_g with a large intensity occurs at 1223.1 cm^{-1} (two modes); this corresponds to an experimental peak at 1225 cm^{-1} . Both of these calculated frequencies are bridge stretching modes. The calculated bridge stretching frequency for D_{2h} 1A_g at 1338.9 cm^{-1} may correspond to a shoulder seen at 1330 cm^{-1} .

Additional results presented in Table 2 illustrate good agreement between calculated terminal hydrogen stretching frequencies and the experimental frequencies. However, the smaller calculated frequencies do not correspond to experimentally reported modes. In particular, those at 1141.3 cm^{-1} (C_s $^1A''$), 1069.4 cm^{-1} (D_{2h} 1A_g), and 1079.6 cm^{-1} (C_{3v} 3E) have significant predicted intensities. It has been suggested that discrepancies between calculations and matrix experiments at the low-frequency end of the spectra are common due to interaction between guest and host molecules.³⁸ In fact, if one considers the broad feature centered at 1250 cm^{-1} in Andrews' argon matrix spectrum⁶ and then looks for the corresponding feature in Margrave's krypton matrix spectrum,⁷ one can see that it has shifted ~110 cm^{-1} to 1140 cm^{-1} . This large shift, which must arise from the different interactions between guest and host in argon versus krypton, is almost zero for higher frequencies.

We conclude that, although definite assignment of experimental peaks based on these calculations is difficult and some

of the good agreement may be fortuitous, the results suggest that Ti_2H_6 could be present. One can make the same conclusion by comparison to Margrave's spectrum. The fact that Margrave's experiment does not produce TiH₃⁷ makes it appropriate to consider alternative pathways to the formation of Ti_2H_6 . Possibilities include $\text{TiH}_2 + \text{TiH}_4 \rightarrow \text{Ti}_2\text{H}_6$ and $\text{Ti}_2\text{H}_4 + \text{H}_2 \rightarrow \text{Ti}_2\text{H}_6$. Andrews et al. showed that there is H-atom participation in their experiment. Since Margrave's experiment did *not* involve H atoms, it is relevant to compare the thermodynamics of the reactions $\text{Ti}_2\text{H}_6 + 2\text{H} \rightarrow \text{Ti}_2\text{H}_8$ and $\text{Ti}_2\text{H}_6 + \text{H}_2 \rightarrow \text{Ti}_2\text{H}_8$ to assess the likelihood of conversion of Ti_2H_6 to Ti_2H_8 on annealing, in the two experiments. Calculated energies of formation can be seen in Table 3 for representative isomers of Ti_2H_6 and Ti_2H_8 . At the best level of theory (MP2 and MCQDPT/TZVP(f)), the reactions with H atoms are highly favorable (–81.9 and –85.1 kcal/mol); however, the reactions with H₂ are thermodynamically unfavorable (+18.6 and +15.5 kcal/mol). This would suggest that, on annealing in Andrews' experiment, conversion of Ti_2H_6 to Ti_2H_8 would be probable. Such a conversion would be much less likely in the Margrave experiment.

(c) Bonding in Ti_2H_6 . We now examine the bonding characteristics of Ti_2H_6 in more detail, paying particular attention to the prototypical D_{2h} $\text{H}_2\text{Ti}(\mu\text{-H})_2\text{TiH}_2$ structure.

Localized Orbitals. The energy localization method of Edmiston and Ruedenberg³⁹ was used to localize the orbitals for all isomers. The localized orbitals (LMOs) clearly show the presence of titanium-terminal hydrogen σ bonds, and Ti–H–Ti three-center, two-electron bonds. Representative plots may be seen in Figure 5a. The LMOs also clearly show two nonbonded electrons in each isomer (see Figure 5b for representative plots). The D_{2h} and D_{4h} isomers are clearly diradical in nature, with one electron localized on each titanium center for singlets as well as triplets. For the singlet and triplet C_{3v} isomers, the nonbonded electrons are found on the three-coordinated titanium center and the three LMOs which represent these electrons are symmetrically equivalent. As the unpaired electrons in the C_s isomers are already localized on each Ti center in the canonical orbital plots (see Figure 4a), one on each titanium center, the LMO plots are not shown.

No strong Ti–Ti bond exists in any of the Ti_2H_6 singlet isomers, even though the Ti–Ti separation is small and two electrons are available. Now, consider the absence of a Ti–Ti bond in the D_{2h} singlet structure, in which the two electrons occupy the bonding σ and antibonding σ^* orbitals almost equally with natural orbital occupation numbers of 1.11 and 0.89 electrons, respectively. Recall that the triplet is higher in energy than the singlet by only ~1 kcal/mol. Intuitively, this reluctance to form a σ bond is somewhat surprising, so the localized charge distribution (LCD) analysis⁴⁰ is used in the following paragraphs in an attempt to provide an interpretation.

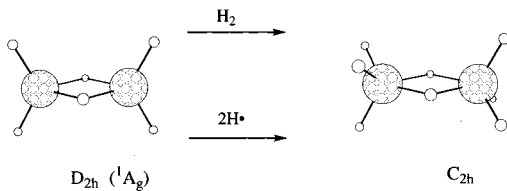
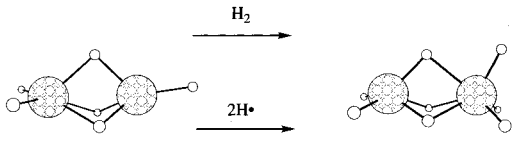
LCD Energy Analysis. It is possible to force the formation of a Ti–Ti σ bond by requiring all orbitals in the singlet to contain two electrons, i.e. an RHF singlet with a doubly occupied Ti–Ti σ bond orbital as the HOMO. At the diradical ROHF geometry, this RHF bonded species is energetically destabilized with respect to the diradical by ~125 kcal/mol. If the RHF geometry is allowed to relax, the Ti–Ti bond shortens by ~0.5 Å and the destabilization energy is reduced to ~98 kcal/mol. Since this is still very large, the energy decomposition and the density difference plots which require the two species

(39) Edmiston, C.; Ruedenberg, K. *Rev. Mod. Phys.* **1963**, 35, 457.

(40) a) Jensen, J. H.; Gordon, M. S. *Acc. Chem. Res.* **1996**, 29, 536. (b) Jensen, J. H.; Gordon, M. S. *J. Phys. Chem.* **1995**, 99, 8091. (c) England, W.; Gordon, M. S. *J. Am. Chem. Soc.* **1971**, 93, 4649.

(38) Kaupp, M.; Schleyer, P. R. *J. Am. Chem. Soc.* **1993**, 115, 11202.

Table 3. Thermodynamics of Reactions $Ti_2H_6 + H_2 \rightarrow Ti_2H_8$ and $Ti_2H_6 + 2H \rightarrow Ti_2H_8$ for Selected Isomers of Ti_2H_6 and Ti_2H_8 ^a

		MCSCF/RHF		MCQDPT/MP2	
		TZVP	TZVP(1)	TZVP	TZVP(1)
 $D_{2h} (^1A_g)$	H_2	+73.6	+71.0	+19.9	+15.5
	$2H\bullet$	-10.8	-13.5	-78.0	-81.9
 $C_s (^1A')$	H_2	+72.7	+70.0	+22.5	+18.6
	$2H\bullet$	-9.8	-12.5	-80.6	-85.1

^a The MCSCF and MCQDPT methods are used for Ti_2H_6 , the RHF and MP2 methods for Ti_2H_8 . Energies are in kcal/mol.

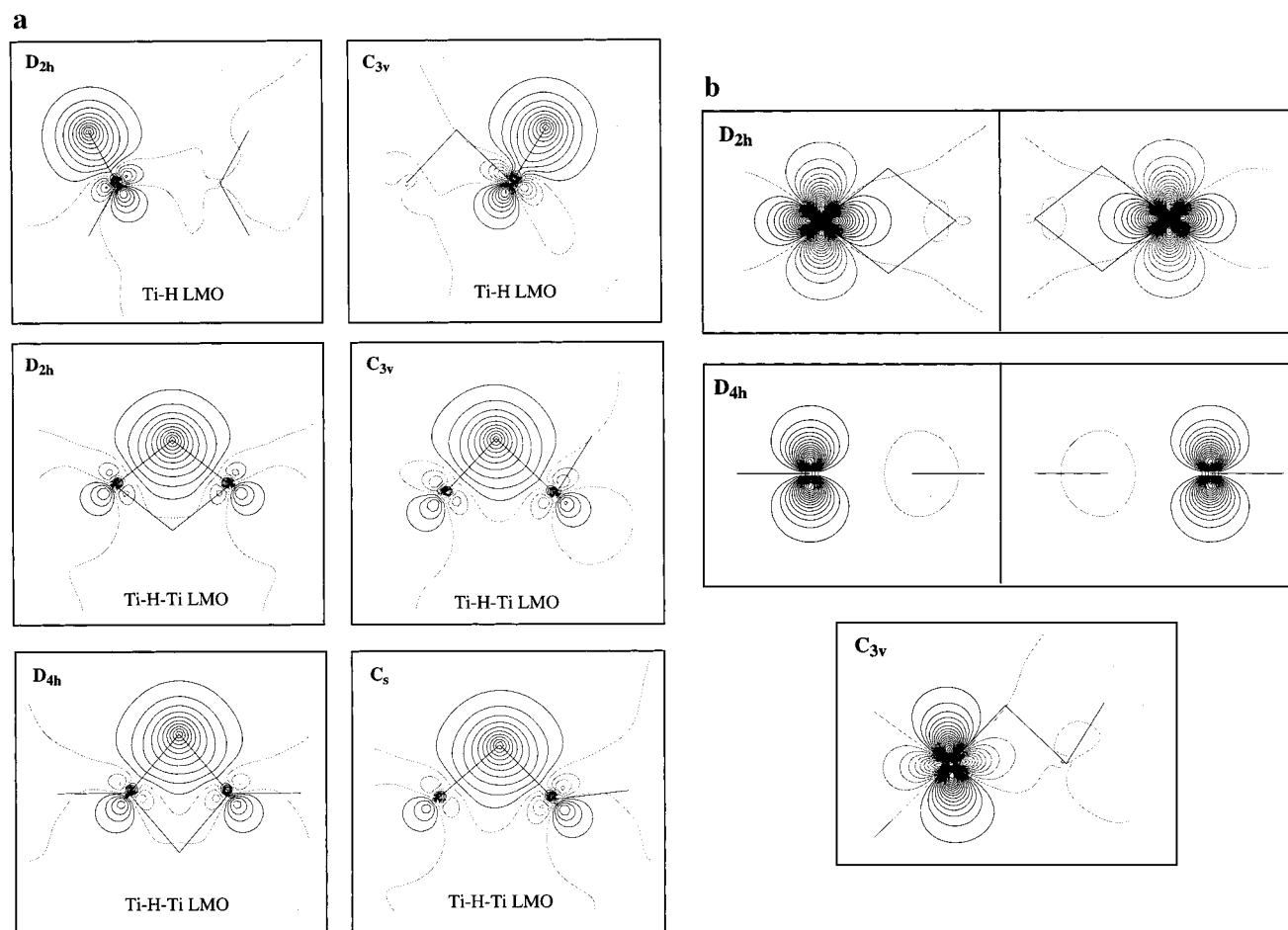
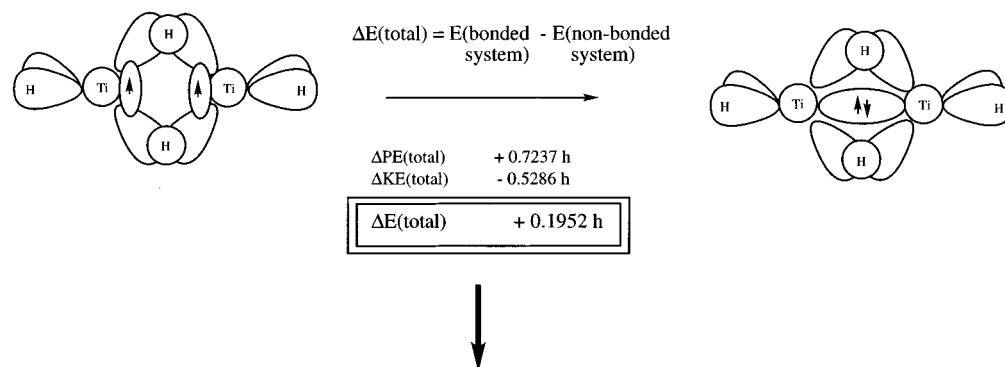


Figure 5. (a) Localized orbital plots showing representative titanium-terminal hydrogen bonds and titanium-hydrogen-titanium bridging bonds in the isomers of Ti_2H_6 . (b) Localized orbital plots showing unpaired/nonbonded electrons for D_{2h} , D_{4h} , and C_{3v} Ti_2H_6 isomers. Singlet and triplet plots are qualitatively the same so only one set for each structure is shown. For D_{4h} the two d-orbital lobes with opposite phase are in the plane perpendicular to the page. Only one of three equivalent plots is shown for the C_{3v} isomer. Contour increments are 0.05 bohr^{3/2}.

to have identical geometries are analyzed at the diradical geometry.

The LCD analysis decomposes the total energy into potential and kinetic energies of LMOs and the interactions between them. Using this analysis for both the bonded and diradical system, it

is possible to track the origin of the destabilization of the bonded system. As the LCD analysis is only implemented for single-configuration wave functions we compare the RHF singlet (bonded species) with the ROHF triplet (purely diradical) at the ROHF triplet geometry (see Figure 1).



LCD analysis used to decompose this energy difference $\Delta E(\text{total})$ into contributions from:

- 1) bond formation ($\Delta PE(\text{bond})$ and $\Delta KE(\text{bond})$)
- 2) rearrangement of remaining electrons in the rest of the molecule ($\Delta PE(\text{internal})$ and $\Delta KE(\text{rest})$)
- 3) bond/unpaired electrons interacting with the rest of the molecule ($\Delta PE(\text{interaction})$)

Figure 6. LCD energy analysis strategy for $\text{H}_2\text{Ti}(\mu\text{-H})_2\text{TiH}_2$. $\Delta E(\text{total})$ is energy difference (in hartrees) between the system constrained to have a Ti–Ti bond and the nonbonded diradical triplet system.

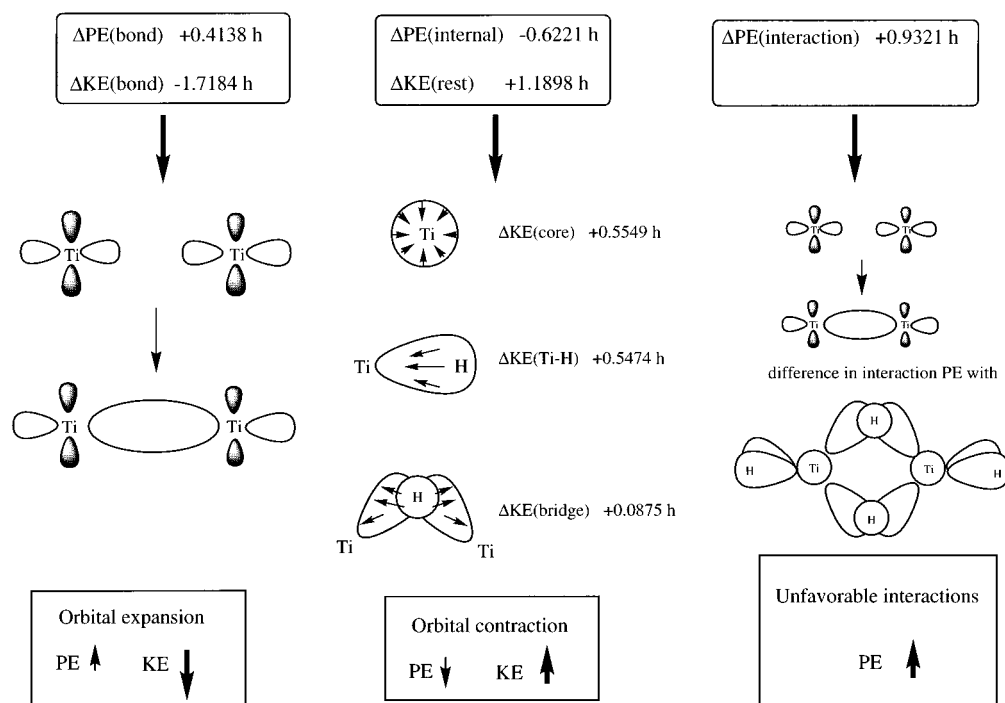


Figure 7. LCD analysis breakdown of $\Delta E(\text{total})$ and schematic explanations of energy increases and decreases. Small arrows within orbitals indicate movement of electrons when a Ti–Ti bond is formed.

In the LCD procedure one assigns a local nuclear charge distribution to each LMO. This was done according to the recommendations of Jensen and Gordon:⁴⁰ for Ti inner shell LMOs (core electrons) Ti was assigned a nuclear charge of 2, for the terminal Ti–H bond LMOs Ti and H were each assigned a nuclear charge of 1, and for the Ti–H–Ti bridging LMOs H was assigned a nuclear charge of 1 and each Ti was assigned a nuclear charge of 0.5.

An overview of the LCD decomposition strategy is shown in Figure 6. The total energy difference (in hartrees) between the bonded species and the nonbonded diradical species is given by $\Delta E = E(\text{bonded system}) - E(\text{nonbonded system})$. From Figure 6 the total energy difference $\Delta E(\text{total})$ is + 0.1952 h, indicating overall destabilization of the molecule on formation of a Ti–Ti bond. This may be decomposed into changes in potential energy ($\Delta PE = + 0.7237 \text{ h}$) and kinetic energy ($\Delta KE = -0.5286 \text{ h}$). So, overall, bond formation produces a

favorable lowering of the KE, but this is more than offset by an increase in PE. A more detailed decomposition leads to the five contributions to ΔE outlined at the bottom of Figure 6: $\Delta PE(\text{bond})$, $\Delta KE(\text{bond})$, $\Delta PE(\text{internal})$, $\Delta KE(\text{rest})$, and $\Delta PE(\text{interaction})$. Figure 7 groups these terms according to their physical significance: (a) bond formation; (b) rearrangement of core, terminal Ti–H and Ti–H–Ti bridge electrons; and (c) interaction of the unpaired electrons/bond electrons with the rest of the molecule.

First consider PE and KE differences between the bond electrons in the Ti–Ti bonded system and the unpaired electrons in the nonbonded system, i.e. the energy difference directly due to bond formation from the two unpaired electrons. The PE term arises from internal energy, except for the very small (–0.0006 h) unpaired electron–unpaired electron interaction energy. The values for $\Delta PE(\text{bond})$ and $\Delta KE(\text{bond})$ are +0.4138 and –1.7184 h, respectively, resulting in a net stabilizing effect

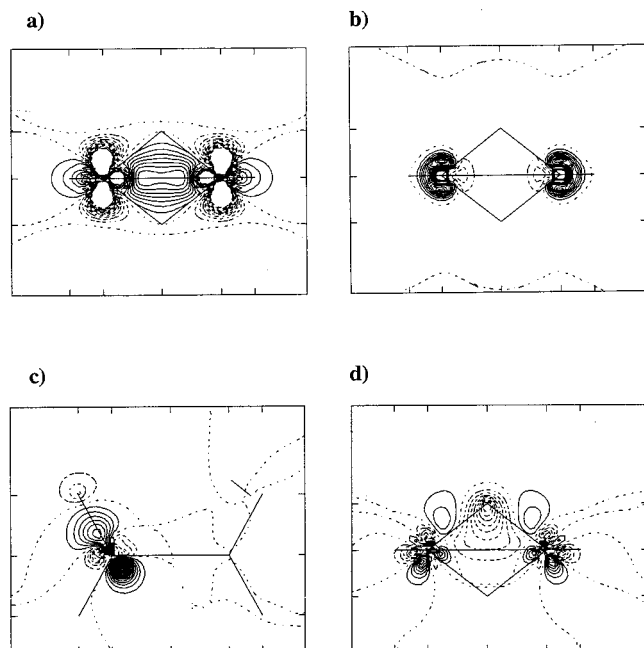


Figure 8. Density difference plots for (a) The Ti-Ti bond; (b) the Ti core electrons, (c) a terminal Ti-H bond, and (d) a Ti-H-Ti bridging bond. These plots represent the RHF Ti-Ti bonded system's density minus the ROHF triplet's density. For a and b, contour increments are 0.002 bohr³; for c and d, contour increments are 0.001 bohr³.

of -1.3046 h. The density difference plot in Figure 8a, the RHF bond density minus the density of the unpaired electrons in the nonbonded triplet, clearly shows a buildup of electron density between the Ti centers. The depletion of electron density from the atomic centers into the bond region decreases the attractive electron-nuclear interaction (increases PE) and decreases the KE by decreasing the curvature of the electron density. A schematic representation of this is given in Figure 7. So, the changes in the bond region itself favor bond formation due to KE lowering. This is entirely consistent with the Ruedenberg interpretation of covalent bonding⁴¹ and with the origin of hydrogen bond formation suggested by Jensen and Gordon.^{40a,b}

Next, consider the PE and KE changes which occur because of electron rearrangement in the rest of the molecule (the core, the terminal Ti-H bonds, and the two Ti-H-Ti bridges) upon bond formation. The term $\Delta E(\text{internal})$ includes self-interactions and interactions among the core, the terminal Ti-H bonds, and the bridges. $\Delta PE(\text{internal})$ and $\Delta KE(\text{rest})$ are -0.6221 and $+1.1898$ h, respectively, resulting in a net destabilization of $+0.5677$ h. The origin of $\Delta PE(\text{internal})$ and $\Delta KE(\text{rest})$ may be found from density difference plots. Figures 8b and 8c illustrate a buildup of electron density around the titanium atoms in the core and Ti-H bonds, respectively. This contraction of the orbitals around the Ti atoms explains the large increase in KE for the core and the Ti-H bonds ($+0.5549$ and $+0.5474$ h, respectively). Figure 8d shows depletion of electron density from directly around the hydrogen in the bridge bond and a corresponding buildup closer to the Ti atoms. The KE decrease due to this orbital expansion around the hydrogen and the KE increase due to the corresponding contraction around the titaniums nearly cancel, resulting in the relatively small change in KE of the bridge of $+0.0875$ h. We do not decompose $\Delta PE(\text{internal})$ for the sake of simplicity, but it is clear that orbital contractions which are responsible for the increase in KE also

produce a corresponding decrease in PE though the KE term dominates. Again, a schematic representation of this can be seen in Figure 7.

Next, consider differences in PE interactions of the bond and the unpaired electrons with the core, Ti-H bond, and the bridges. The LCD analysis shows $\Delta PE(\text{interaction})$ to be $+0.9321$ h, a large destabilizing effect with all the above interactions making a significant positive contribution. These unfavorable interactions produced by electron-electron repulsion are, in fact, large enough to outweigh the stabilizing effect of the first four terms ($\Delta PE(\text{bond}) + \Delta KE(\text{bond}) + \Delta PE(\text{internal}) + \Delta PE(\text{rest}) = -0.7369$ h) and produce a net destabilization $\Delta E(\text{total}) = +0.1952$ h on bond formation.

In summary, to form a Ti-Ti σ bond in $H_2Ti(\mu-H)_2TiH_2$ requires the depletion of electronic density from around the Ti's and a buildup of charge between them. The potential energy of these two electrons is increased and their kinetic energy is lowered, the kinetic energy term dominating. The remaining electrons contract around the titaniums driving up the kinetic energy and lowering the potential energy, the kinetic energy term dominating. The net effect of these interactions favor bond formation ($\Delta PE(\text{bond}) + \Delta KE(\text{bond}) + \Delta PE(\text{internal}) + \Delta KE(\text{rest}) = -0.7369$ h); however, the increase in potential energy produced by the unfavorable interaction of the bond with the rest of the molecule ($\Delta PE(\text{interaction}) = +0.9321$ h) is large enough to ultimately ensure net destabilization upon bond formation (by $+0.1952$ h). One simple interpretation here is that there is no σ bond in $H_2Ti(\mu-H)_2TiH_2$ due to steric repulsions between the bond and the rest of the molecule.

Mulliken Populations. MCSCF and ROHF Mulliken populations with the TZVP basis set show positively charged Ti's and negatively charged H's for all isomers (both singlet and triplet). Charges range from $\sim +0.6$ to $\sim +0.8$ on the Ti's and ~ -0.1 to ~ -0.3 on the hydrogens. These charges indicate considerable bond polarization in Ti_2H_6 .

(d) Magnetic Properties of D_{2h} $H_2Ti(\mu-H)_2TiH_2$. Magnetic properties of molecular systems comprising dinuclear complexes which have a single unpaired electron on each metal center depend strongly on the intramolecular interaction of the metal centers with each other. This interaction itself can be affected by perturbations due to bridging and terminal ligands. If the singlet state is lowest in energy the interaction is antiferromagnetic; if the triplet state is lowest in energy the interaction is ferromagnetic.²² Here we focus on the D_{2h} Ti_2H_6 structures, since they are the most closely related to experimentally known compounds.

The isotropic interaction between metal centers in these dinuclear complexes is reflected by the calculated singlet-triplet energy gap, where effects of spin-orbit coupling and magnetic dipole-dipole interactions are neglected. The isotropic effect has been found to be highly dominant in determining the magnetic interactions in dititanium molecules studied experimentally^{17,18} and is the only effect considered here. Results of a study on the much smaller spin-orbit coupling effects²² will be presented elsewhere.⁴² To be consistent with most of the experimental work referenced, we define the isotropic interaction parameter J by $-2J = E(\text{triplet}) - E(\text{singlet})$. Inclusion of dynamic as well as nondynamic correlation effects is known to be essential to obtain reliable calculated singlet-triplet energy gaps in paramagnetic dinuclear complexes. A method which has achieved some success is "dedicated-difference configuration

(41) Ruedenberg, K. *Rev. Mod. Phys.* **1962**, *34*, 326.

(42) Webb, S. P.; Gordon, M. S. *J. Chem. Phys.*, submitted.

Table 4. Calculated Singlet–Triplet Energy Gap ($E(\text{triplet}) - E(\text{singlet})$) for D_{2h} $\text{H}_2\text{Ti}(\mu\text{-H})_2\text{TiH}_2$ in kcal/mol

basis set	method of singlet/triplet calculation	
	MCSCF/ROHF	MCQDPT/MCQDPT
TZVP	0.56	1.33
TZVP(f)	0.56	1.40
TZVP(f,g)	0.56	1.43

interaction” (DDCI2).⁴³ This CISD method (which is applicable to any multiplet splitting) calculates the singlet–triplet energy gap directly at one geometry, using the same reference orbitals for singlet and triplet (usually ROHF triplet geometry and orbitals). This reduces the number of configurations in the variational CISD, as many of these configurations make exactly the same contribution to the energy of both multiplicities. This method is a relatively inexpensive way of including dynamic correlation and has been effective in predicting singlet–triplet energy gaps in compounds such as $[\text{Cu}_2\text{Cl}_6]^{2-}$ and $[\text{Ni}(\text{NH}_3)_4\text{Cl}]_2^{2+}$ in qualitative and, to some degree, quantitative agreement with experiment.⁴⁴ In the present study, a more quantitatively correct method is used.

We determine the singlet–triplet energy gap in D_{2h} $\text{H}_2\text{Ti}(\mu\text{-H})_2\text{TiH}_2$ by calculation of the singlet and triplet energies separately. These are single-point MCQDPT energies at the geometries and reference wave functions of the TCSCF singlet and the ROHF triplet. Therefore, orbital and geometry relaxation effects are included. Table 4 shows the calculated values of the singlet–triplet energy gap in D_{2h} $\text{H}_2\text{Ti}(\mu\text{-H})_2\text{TiH}_2$. It is clear from Table 4 that basis set convergence is very rapid, suggesting large cancellation of error. At the MCSCF/TZVP-(f,g) and ROHF/TZVP(f,g) levels the singlet 1A_g state is predicted to be lower in energy than the triplet $^3B_{3u}$ state by 0.56 kcal/mol ($J = -98 \text{ cm}^{-1}$), due to the small Ti–Ti bonding interaction discussed earlier. As expected, the inclusion of dynamic correlation stabilizes the singlet preferentially to the triplet as the ROHF wave function already contains like-spin electron correlation. MCQDPT/TZVP(f,g) predicts that singlet 1A_g is lower in energy than triplet $^3B_{3u}$ by 1.43 kcal/mol ($J = -250 \text{ cm}^{-1}$). The intramolecular metal–metal interaction in D_{2h} $\text{H}_2\text{Ti}(\mu\text{-H})_2\text{TiH}_2$ is therefore predicted to be antiferromagnetic. As neglect of dynamic correlation (MCSCF) already results in an antiferromagnetic interaction, it is unlikely that a more sophisticated treatment of dynamic correlation than MCQDPT will change the sign of J . Review of the literature supports this, given that MCSCF generally underestimates the size of the antiferromagnetic interaction in these types of systems.^{23,45}

To assess the effect of neglecting geometry and orbital relaxation, calculations were repeated with both singlet and triplet at the triplet geometry; first allowing orbital relaxation in the singlet calculation and then using the “frozen” ROHF orbitals for the singlet calculation. Constraining both geometries to that of the triplet lowered the singlet–triplet energy gap by 0.05 and 0.30 kcal/mol without and with dynamic correlation, respectively. The additional effect of neglecting orbital relaxation lowered the gap by a further 0.15 and 0.04 kcal/mol without and with dynamic correlation, respectively. These effects are not negligible in terms of wavenumbers (0.34 kcal/mol corresponds to $J = 60 \text{ cm}^{-1}$).

(43) Handrick, K.; Malrieu, J. P.; Castell, O. *J. Chem. Phys.* **1994**, *101*, 2205.

(44) (a) Castell, O.; Miralles, J.; Caballol, R. *Chem. Phys.* **1994**, *179*, 377. (b) Castell, O.; Caballol, R.; García, V. M.; Handrick, K. *Inorg. Chem.* **1996**, *35*, 1609.

(45) Fink, K.; Fink, R.; Staemmler, V. *Inorg. Chem.* **1994**, *33*, 6219.

The singlet–triplet splitting energy in D_{2h} $\text{H}_2\text{Ti}(\mu\text{-H})_2\text{TiH}_2$ is for the homodinuclear titanium(III) system in which interactions of the Ti centers with bridging and terminal ligands is *minimal* and the Ti–Ti $\sigma\text{-}\sigma$ ground state isotropic interaction is the least perturbed by its environment. The most closely related experimentally characterized compound is *rac*- $\{[\text{C}_2\text{H}_4(\eta^5\text{-tetrahydroindenyl})_2]\text{-Ti(III)}(\mu\text{-H})\}_2$,¹³ which also has bridging hydrogens. It exhibits antiferromagnetic behavior (no value for J is reported; only the sign) in line with our prediction for D_{2h} $\text{H}_2\text{Ti}(\mu\text{-H})_2\text{TiH}_2$. The experimentally measured antiferromagnetic singlet–triplet splitting in $[\text{Cp}_2\text{Ti}(\mu\text{-OCH}_3)]_2$ is $1.53 \pm 0.02 \text{ kcal/mol}$ ($J = -268 \pm 4 \text{ cm}^{-1}$)¹⁸ very close to the calculated value of 1.43 kcal/mol for D_{2h} $\text{H}_2\text{Ti}(\mu\text{-H})_2\text{TiH}_2$. Superficially this may indicate that effects due to bridging ligands, terminal ligands, and Ti–Ti separation, which is 3.35 Å in $[\text{Cp}_2\text{Ti}(\mu\text{-OCH}_3)]_2$ and 3.04 Å in D_{2h} $\text{H}_2\text{Ti}(\mu\text{-H})_2\text{TiH}_2$, are small. However, even if one is to trust that the calculated value is accurate enough for such a comparison, it may indicate opposing effects which cancel each other in this case, considering that replacement of the ($\mu\text{-OCH}_3$) bridging ligands with ($\mu\text{-Cl}$) ligands^{18,17} results in a experimentally determined value of $J = -111 \text{ cm}^{-1}$ ($S\text{-T}$ gap of 0.63 kcal/mol) and replacement with ($\mu\text{-O}$) will even change the sign of the interaction ($J = +8 \text{ cm}^{-1}$). Thus, future work will focus on the effect of systematic replacement of bridging and terminal hydrogens with other species on the fundamental electronic structure of this system, to establish trends allowing prediction and therefore modification of the magnetic properties of molecules. This seems a reasonable goal given that prediction of trends is easier than prediction of absolute J values.

IV. Conclusions

Five singlet and five triplet minima were found on the two lowest potential energy surfaces of Ti_2H_6 , all with bridging hydrogens. The ($\mu\text{-H}$)₃ C_{3v} staggered and eclipsed structures, which have been described in the past by a closed shell RHF reference wave function, actually require a two-electron, three-orbital FORS-MCSCF reference wave function; the triplet structures require an ROHF reference wave function in which two degenerate states are averaged. The remaining minima are adequately described with TCSCF or ROHF reference wave functions.

No Ti–Ti bonding is possible in the triplet minima. More surprising is the prediction there is little or no Ti–Ti bonding in the singlet minima as well. In the ($\mu\text{-H}$)₃ C_{3v} minima both of the nonbonded electrons are found on the least saturated Ti. The ($\mu\text{-H}$)₃ C_s minima ($^1A''$ and $^3A''$) are both purely diradical. Natural orbital analysis of the wave functions of the ($\mu\text{-H}$)₂ D_{2h} singlet and the ($\mu\text{-H}$)₄ D_{4h} singlet show a large amount of diradical character, although a slight bonding interaction is predicted in the D_{2h} and D_{4h} singlets. This is supported by calculated singlet–triplet splittings of 1.3 and 1.4 kcal/mol for the D_{2h} and D_{4h} structures, respectively. All minima are predicted to be lower in energy than 2TiH_3 . The triplet C_s structure is the lowest in energy with an exothermic dimerization energy of 56.4 kcal/mol on the classical potential energy surface and 52.0 kcal/mol on the adiabatic ground-state surface (zero-point energy correction included). Inclusion of dynamic correlation is found to be important, its effects being especially large for the ($\mu\text{-H}$)₃ and ($\mu\text{-H}$)₄ structures.

Comparison of calculated frequencies of representative Ti_2H_6 isomers with the experimental spectra of Andrews et al. suggests that the presence of Ti_2H_6 in the matrix is entirely possible. The same conclusion may be reached by comparison of calculated

frequencies to the spectra of Margrave et al. In Margrave's experiment TiH_3 is not observed, suggesting a route to Ti_2H_6 other than the dimerization of TiH_3 . $TiH_2 + TiH_4 \rightarrow Ti_2H_6$ and $Ti_2H_4 + H_2 \rightarrow Ti_2H_6$ are suggested as possibilities. The absence of H atoms in the Margrave experiment will reduce the likelihood of the hydrogenation reaction $Ti_2H_6 \rightarrow Ti_2H_8$ on annealing, due to unfavorable thermodynamics when the reaction occurs with H_2 .

Localized orbital plots of the terminal Ti–H and bridging Ti–H–Ti bonds are much the same as those seen in Ti_2H_8 . The lack of Ti–Ti bonding in C_s , D_{4h} , and C_{3v} singlets may be rationalized in terms of location of electrons, symmetry, and orientation of d orbitals. This is not the case for the D_{2h} singlet, which appears ideally suited to Ti–Ti σ bond formation. An LCD energy analysis suggests that the lack of Ti–Ti bonding in the D_{2h} isomer arises due to steric crowding, i.e. unfavorable interactions of the bond with the surrounding molecule.

The D_{2h} $H_2Ti(\mu-H)_2TiH_2$ structure is an excellent prototype for the many homodinuclear titanium(III) compounds known experimentally. A good example is titanocene dimer $[(\eta^5-C_5H_5)Ti(\mu-H)]_2(\mu-\eta^5:\eta^5-C_{10}H_8)$. Experimental evidence suggests either a Ti–Ti bond or a large singlet–triplet energy gap in this compound. Since we find no such bond in $H_2Ti(\mu-H)_2TiH_2$ and a very small singlet–triplet energy gap, it appears that the presence of the cyclopentadienyl rings and/or the distortion of the bridge out of the plane must modify the electronic structure in such a way that bond formation is facilitated or the singlet is stabilized significantly, preferentially to the triplet. This is the subject of an ongoing study.

Paramagnetic homodinuclear titanium(III) compounds for which the singlet is lower in energy than the triplet are antiferromagnetic. If the triplet is lower in energy than the singlet, the compound is ferromagnetic. By this criterion, we find $H_2Ti(\mu-H)_2TiH_2$ to be antiferromagnetic and conclude that this is due to a small bonding interaction between Ti's in the singlet (isotropic interaction).

Acknowledgment. This work was supported by a grant from the National Science Foundation (CHE-9633480). The calculations reported here were performed on IBM RS 6000 workstations generously provided by Iowa State University. The authors thank Dr. Michael Schmidt for many informative discussions and Dr. Jan Jensen for help and advice concerning the LCD energy analysis.

Appendix

(a) Jahn–Teller Effects in Singlet C_{3v} Ti_2H_6 Isomers. To test for Jahn–Teller effects, the geometry of the 1A_1 C_{3v} eclipsed isomer (see section IIb) was distorted slightly from C_{3v} to C_s symmetry. Orbital symmetry constraints requiring degenerate e levels were therefore removed and a two-electron, three-orbital MCSCF geometry optimization was carried out on this ${}^1A'$ state with a' , a' , and a'' orbitals active. The resulting optimized geometry returned to essentially C_{3v} symmetry, and the energy of this structure was lower by only 0.5 kcal/mol, suggesting negligible Jahn–Teller distortion.

If the two 1E configurations which make up the first excited singlet state (see section IIb) are not averaged, the result is occupation of only one of a pair of degenerate e orbitals (see Figure 2a), and this may lead to Jahn–Teller distortions to C_s structures. The question of Jahn–Teller distortion is again addressed by relaxing symmetry constraints to C_s , thereby splitting the degenerate e orbitals into a' and a'' . The “state-averaged” 1E excited state is therefore split into a ${}^1A'$ state (two singly occupied a' orbitals) and a ${}^1A''$ state (a singly occupied a' and a singly occupied a''). The ${}^1A'$ state is actually a configuration included in the two-electron, three-orbital calculation described in the previous paragraph and is not considered further. A singlet ROHF geometry optimization performed on the ${}^1A''$ state indicated no appreciable geometry change, and the resulting structure is almost isoenergetic with the C_{3v} 1E state, with a decrease in energy of only 0.3 kcal/mol. As in the ground state, Jahn–Teller distortion is therefore considered to be unimportant.

(b) Jahn–Teller Effects in Triplet C_{3v} Ti_2H_6 Isomers. To assess the possibility of Jahn–Teller distortion of the 3E state (section IIb and Figure 2b), symmetry constraints were relaxed to C_s . Two ROHF/TZVP geometry optimizations were carried out on the eclipsed structure, one with two a' orbitals singly occupied (${}^3A'$) and one with a'' and a' each singly occupied (${}^3A''$). Negligible geometry and energy changes (energy decrease of 0.4 kcal/mol for both ${}^3A'$ and ${}^3A''$) occurred, indicating no Jahn–Teller distortion.

Supporting Information Available: Calculated total energies of TiH_3 ${}^2A'_1$ state (1 page, print/PDF). See any current masthead page for ordering and Web access instructions.

JA973195S